NON LOCAL MEANS IMAGE DENOISING USING NOISE-ADAPTIVE SSIM

V. Bruni

University of Rome "La Sapienza"
Dept. of SBAI
Via A. Scarpa 16, 00161 Rome, Italy
e-mail: vittoria.bruni@sbai.uniroma1.it.

D. Panella, D. Vitulano

National Research Council
IAC "M. Picone"
via dei Taurini 19, 00185 Rome, Italy
e-mail: d.vitulano@iac.cnr.it

ABSTRACT

This paper embeds SSIM in place of the L_2 norm in a one step Non Local Means (NLM) scheme. This is possible thanks to a new form of SSIM that can be formally derived from the classical SSIM using the spreading error analysis. This approach has several advantages over L_2 norm based NLM such as greater robustness to parameters setting, higher performance in terms of PSNR and SSIM, optimal subjective visual quality. In addition, it is possible to show that the cascade of the proposed pure visual approach and a second step based on L_2 norm allows us to reach results close (slightly less) to the state of the art (BM3D) in terms of PSNR and SSIM.

Index Terms— Image denoising, Non Local Means, SSIM, Wiener filter.

1. INTRODUCTION

Image denoising is fundamental in various application fields like image acquisition, quantization, transmission and so on. Among the plethora of approaches proposed in the literature, Non-Local Means (NLM) [1] is probably the one which has received the major interest in the last years. The main reason stems from the fact it is based on a simple, formal and very performing idea: any noisy pixel can be cleaned using a weighted sum of noisy pixels having similar neighborhood located everywhere in the image. The more similar the neighborhood (patch), the higher the weight for the corresponding pixel. Apart from approaches that used NLM for specific applications (see for instance [18, 19]), many papers proposed different solutions to overcome NLM's weak points oriented to: *i)* speed up NLM process [2–5], *ii)* make NLM more robust to parameters setting like the smoothing parameter in the weight function and the adopted similarity window dimension [6, 7] and *iii)* make NLM more performing and competitive with the state of the art (i.e. BM3D [13]) [5, 8–12].

All the aforementioned approaches make use of the L_2 norm (or equivalently, Mean Square Error (MSE)) for evaluating the distance between image patches. That is why in the sequel classical NLM will be denoted with MSE-NLM. However, despite the historical use of MSE as similarity metric, it is well known that MSE is not the best candidate when the perceived image quality is the final target [15]. More recently, the structural similarity (SSIM) index [16] has been proposed as an alternative image quality assessment metric in order to meet human visual system behavior. Several studies and applications in image processing have shown its better performance over MSE.

A first attempt to replace MSE with SSIM has been proposed in [14] (that will be indicated with SSIM-NLM). Authors showed that SSIM cannot straightforwardly be used into a NLM scheme as it is very sensitive to noise. It turns out that the noisy image is firstly cleaned by a MSE-NLM process and then patches from the cleaned image are used for the computation of NLM weights. Even though the good SNR performance, such an approach has various drawbacks when compared to MSE-NLM: *i)* it is less desirable from the computing time point of view since a two step framework is required; *ii)* involved precleaning and normalization lead to lose 'a pure' visual denoising as still tied to MSE.

This paper proves that SSIM can be embedded in a one step NLM denoising scheme. A simple but slightly different form of SSIM is adopted in the case of not correlated noise. It is mathematically derived from the classical SSIM by evaluating how the noise affecting the original image spreads over the measure. The main advantages of this approach, that will be called Adaptive SSIM-NLM (ASSIM-NLM), can be summarized as follows:

1. greater robustness to the adopted parameters (smoothing factor, blocks dimension) if compared to MSE-NLM;
2. higher performance in terms of PSNR and SSIM than the (one step) MSE-NLM as well as its variants like median based NLM [12];
3. better subjective visual quality of the denoised image. In other words, many artifacts in the recovered image, that led to ad hoc approaches [11], are automatically avoided;
4. high flexibility: it allows us to employ the same methods (like [17]) used for improving MSE-NLM as well as to define a two step denoising framework.

It is worth outlining the last point. In fact, the proposed frame-

978-0-9928626-3-3/15/$31.00 ©2015 IEEE

work uses a 'pure' visual perception based criterion for selecting similar patches. It is then possible to combine a second MSE based phase to also exploit the complementary L_2 based criterion to increase denoising performance. A simple example based on Wiener filter at the end of the next section shows this possibility. The proposed two-step method will be denoted with I-ASSIM-NLM (Improved Adaptive SSIM based NLM) and it is able to reach denoising results that are slightly less but close to those of BM3D.

The outline of the paper is the following. The next section presents the proposed correction to SSIM and its embedding in the NLM algorithm. A further refinement of denoising results is also proposed. Section 3 presents some experimental results achieved on some test images and for different levels of noise. Comparative studies with the state of the art denoising methods have also been provided. Concluding remarks and guidelines for future research are the topic of the last section.

2. THE PROPOSED MODEL

Classical NLM uses MSE as similarity metric between two image patches. In particular, at each pixel location $\mathbf{x}$ the value of the original image I is estimated as a weighted average of the values of the noisy image J (with $J = I + N$, where N is i.i.d. zero mean additive gaussian noise with variance σ^2) corresponding to the pixels belonging to a window W (search window) centered at $\mathbf{x}$ and of a certain size (in principle it may be the whole image size), i.e. $I_{NLM}(\mathbf{x}) = \sum_{\mathbf{y}\in W} w_y J(\mathbf{y})$, where the weights w_y are estimated as follows

$$w_y = e^{(-\frac{\|J(B_{\mathbf{x}})-J(B_{\mathbf{y}})\|_2^2}{h})} \tag{1}$$

and $B_{\mathbf{x}}$ and $B_{\mathbf{y}}$ are the adopted similarity windows (the two blocks to be compared) and h is a smoothing parameter. Hence, the more similar $B_{\mathbf{x}}$ and $B_{\mathbf{y}}$ are, the smaller the MSE value, the higher the weight w_y. In other words, similar points contribute more in the weighted average than dissimilar points. In this paper we propose to use SSIM as similarity metric in the definition of the weight w_y. SSIM is defined as follows [16]:

$$S(B_x, B_y) = \underbrace{\frac{2\mu_x\mu_y + C_1}{\mu_x^2 + \mu_y^2 + C_1}}_{S_1} \underbrace{\frac{2\sigma_{xy} + C_2}{\sigma_x^2 + \sigma_y^2 + C_2}}_{S_2} \tag{2}$$

where μ_* and σ_* respectively are the mean value and the standard deviation in B_* while σ_{xy} is the correlation between the values in the blocks B_x and B_y and C_1 and C_2 are two normalizing constants. $\sqrt{1-S_1}$ and $\sqrt{1-S_2}$ are two normalized metrics in $\mathbf{R}^n$ [20]. Unfortunately, as already shown in [14], the straightforward use of SSIM cannot guarantee the same denoising results of the classical NLM. In fact SSIM is too much sensitive to the noise when measuring similarities between noisy blocks. That is why in [14] the noisy image is firstly denoised using MSE-NLM. Such a denoised image is then used for estimating the SSIM-based weights of NLM algorithm.

The main idea of the presented paper is to define a one step denoising algorithm where a corrected version of SSIM is used as similarity measure. Specifically, using a simple algebra, the term $1 - S(B_x, B_y)$ is written in the following equivalent form

$$\begin{aligned}(1 - S(B_x, B_y)) = \\ = (1 - S_1(B_x, B_y)) + (1 - S_2(B_x, B_y))S_1(B_x, B_y).\end{aligned} \tag{3}$$

It is worth observing that, by indicating with $\tilde{*}$ the noisy quantities, the previous equation also holds for the noisy values $\tilde{S}_1$, $\tilde{S}_2$ and $\tilde{S}$. Hence, the main idea is to adopt this form for the computation of SSIM and to correct the estimation of S_1 and S_2 from the noisy data using the error propagation analysis [21]. In general, by indicating with m a given variable and with $\tilde{m}$ its measured version, the relative error ε_m in the approximation by m with $\tilde{m}$ can be written as

$$\varepsilon_m = \frac{\tilde{m} - m}{m} \quad \Rightarrow \quad \tilde{m} = (1 + \varepsilon_m)m.$$

The same identities hold if the roles of m and $\tilde{m}$ are interchanged. It turns out that $\tilde{S}_1$ and $\tilde{S}_2$ depend on the original S_1 and S_2 as follows

$$\begin{aligned}S_1 = \tilde{S}_1(1 + \varepsilon_{\tilde{S}_1}), \qquad S_2 = \tilde{S}_2(1 + \varepsilon_{\tilde{S}_2}), \\ (1 - S_1) = (1 - \tilde{S}_1)(1 + \varepsilon_{1-\tilde{S}_1}), \\ (1 - S_2) = (1 - \tilde{S}_2)(1 + \varepsilon_{1-\tilde{S}_2}),\end{aligned} \tag{4}$$

where $(1 + \varepsilon_*)$ represents the corrective term to apply to the corresponding noisy measure in order to get the true measure $*$. Hence, by applying these corrective terms in eq. (4) in the second member of eq. (3), we get an estimation of the clean value of $1 - S$, i.e.

$$\begin{aligned}(1 - S(B_x, B_y)) = \\ = (1 + \varepsilon_{1-\tilde{S}_1})(1 - \tilde{S}_1(B_x, B_y)) + \\ +(1 + \varepsilon_{1-\tilde{S}_2})(1 - \tilde{S}_2(B_x, B_y))(1 + \varepsilon_{\tilde{S}_1})\tilde{S}_1(B_x, B_y).\end{aligned} \tag{5}$$

Hence, the weights to use in the NLM algorithm are

$$\bar{w}_y = \exp\left(-\frac{1 - S(B_x, B_y)}{h}\right),$$

where $(1 - S(B_x, B_y))$ is computed using eq. (5), and the denoised image is $I_d(\mathbf{x}) = \sum_{\mathbf{y}\in W} \bar{w}_y J(\mathbf{y})$.

Before giving the form of the corrective terms, it is worth observing that the term in SSIM that is more sensitive to noise is S_2, due to its dependence on the correlation coefficient. S_1 depends on the mean values in the image patches and then their estimation is more robust to the presence of noise whenever the size of image patches is not too small. That is why

Fig. 1. Denoising results on Lena and Barbara images for $\sigma = 20$. From left to right: ASSIM-NLM, MSE-NLM
.

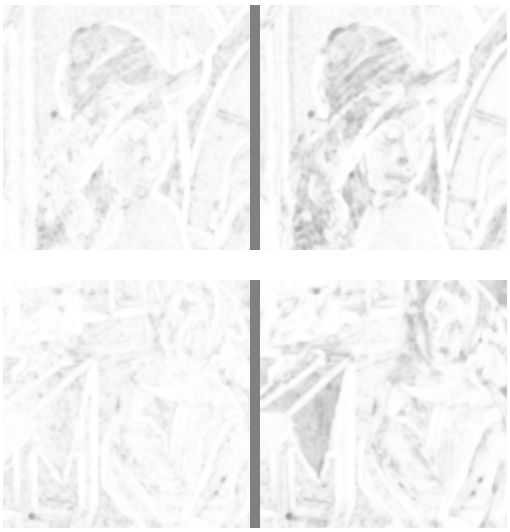

Fig. 2. SSIM maps of the images in Fig. 1. The brighter the pixel the higher the local SSIM value [16].

we can simplify the expression in eq. (5) by neglecting the error of S_1 (i.e. by setting $\varepsilon_{\tilde{S}_1} = \varepsilon_{1-\tilde{S}_1} = 0$) and considering just the error on $1 - S_2$, which has the following form:

$$\varepsilon_{1-\tilde{S}_2} \approx \frac{2\sigma^2}{\|B_x - B_y - (\mu_x - \mu_y)\|^2} + - \frac{2\sigma^2}{\|B_x - \mu_x\|^2 + \|B_y - \mu_y\|^2 + C_2}. \quad (6)$$

Details for the estimation of $\varepsilon_{1-\tilde{S}_2}$ are in the Appendix.

As a matter of fact the predominant role of S_2 is confirmed by the following observation. In ideal conditions, i.e. image patches sufficiently large, there exists a precise relation between S and $\tilde{S}$. Since noise is zero-mean and independent of the image, we have $\mu_* = \tilde{\mu}_*$, $\sigma_*^2 = \tilde{\sigma}_*^2 + \sigma^2$ and $\sigma_{xy} = \tilde{\sigma}_{xy}$, hence $\tilde{S}_1 = S_1$ and then

$$\tilde{S}(B_x, B_y) = \frac{\sigma_{B_x}^2 + \sigma_{B_y}^2 + C_2}{\tilde{\sigma}_{B_x}^2 + \tilde{\sigma}_{B_y}^2 + C_2} S(B_x, B_y).$$

Unfortunately, in case of small blocks (pointwise SSIM estimation), previous relation does not hold because of the instability of the correlation term in S_2. That is why we introduced the corrective term in eq. (8).

2.1. Combining SSIM and MSE: I-ASSIM-NLM

In order to eliminate the residual noise as well as some artifacts introduced in the denoised image I_d, a further denoising step can be performed. In particular, following the strategy suggested in [22], the residual image $R(\mathbf{x}) = J(\mathbf{x}) - I_d(\mathbf{x})$ is computed and a wavelet-based Wiener filtering is applied to both I_d and R. The coefficients of the Wiener filter that is applied to R are computed using I_d as estimation of the original image information. The final denoised image is then $I_d + R_d$, where R_d is the denoised residual. For the denoised image a conventional empirical Wiener filter is applied to each wavelet subband by adjusting the noise variance at each level (i.e., $\frac{\sigma^2}{2^j}$ is the noise variance at the $j-$th level.). It will be shown in the next section that the combination of ASSIM-NLM and an additional simple MSE step allows us to reach results close to the state of the art both in terms of SSIM and PSNR. This is due to the exploitation of two different denoising strategies based on visual perception (SSIM) and data information (MSE).

3. EXPERIMENTAL RESULTS

The proposed denoising method has been tested on several images and different noise levels. Some results are contained in Table 1. They have been achieved using a 19×19 window size for the blocks to be compared and 31×31 as search window. Results do not change if blocks with smaller size are selected. The smoothing parameter has been fixed to $h = 0.02$. Table 1 compares the denoising results of the proposed ASSIM-NLM and MSE-NLM (using the same parameters) in terms of Peak Signal to Noise Ratio (PSNR) and Structural Similarity Index (SSIM). The values in the table are the average over 30 runs of the algorithm. As it can be observed, ASSIM-NLM outperforms MSE-NLM of about $1db$ on average in terms of PSNR and 0.03 in terms of SSIM. It is also worth observing the visual quality of the denoised images. As shown in Fig. 1 the visual appearance of the restored im-

Table 1. $512 \times 512 \times 8bits$ Lena, Barbara, and Boats images. Comparisons in terms of PSNR and SSIM (in the brackets) of denoising results of the proposed ASSIM-NLM, its refined version (I-ASSIM-NLM), MSE-NLM, its refined version (I-MSE-NLM), and BM3D for different noise standard deviations.

Image	Method	Noise StD σ 10	20	30	40
Lena	ASSIM-NLM	34.86 (0.961)	31.61 (0.922)	29.55 (0.886)	27.86 (0.844)
	MSE-NLM	34.43 (0.947)	30.46 (0.890)	28.27 (0.845)	26.81 (0.808)
	BM3D	35.93 (0.969)	33.05 (0.940)	31.26 (0.912)	29.86 (0.884)
	I-ASSIM-NLM	35.57 (0.968)	32.83 (0.939)	30.80 (0.910)	29.70 0.883
	I-MSE-NLM	35.08 (0.962)	31.94 (0.924)	29.96 (0.888)	28.60 (0.856)
Barbara	ASSIM-NLM	33.17 (0.967)	30.50 (0.939)	28.42 (0.903)	26.78 (0.862)
	MSE-NLM	33.30 (0.962)	29.95 (0.899)	26.17 (0.834)	24.41 (0.775)
	BM3D	34.98 (0.977)	31.78 (0.953)	29.81 (0.927)	27.99 (0.894)
	I-ASSIM-NLM	33.97 (0.973)	31.30 (0.950)	29.27 (0.921)	27.90 (0.894)
	I-MSE-NLM	33.30 (0.970)	29.39 (0.921)	26.82 (0.868)	25.11 (0.816)
Boats	ASSIM-NLM	32.70 (0.952)	29.57 (0.891)	27.48 (0.831)	25.97 (0.798)
	MSE-NLM	31.86 (0.922)	27.94 (0.821)	25.63 (0.748)	24.25 (0.693)
	BM3D	33.92 (0.966)	30.88 (0.925)	29.12 (0.887)	27.74 (0.850)
	I-ASSIM-NLM	33.46 (0.965)	30.43 (0.920)	28.44 (0.873)	27.26 (0.822)
	I-MSE-NLM	32.82 (0.951)	29.25 (0.875)	27.13 (0.811)	25.73 (0.759)

ages using the proposed denoiser is very good: the image does not show annoying smoothing effects and textures have been recovered very well. In order to emphasize this aspect, the SSIM image of the recovered image is shown in Fig. 2 and it has been compared with the same SSIM map computed on the results of the classical NLM. As it can be observed the proposed denoising algorithm is able to recover textures of the original image without introducing smoothing. In addition it better preserves some details on the image edges. As it is evident in Fig. 3, the proposed one step ASSIM-NLM allows us to reach the same results of the two step SSIM-NLM in [14] with a considerable computing time saving. In fact, with respect to MSE-NLM, the proposed denoiser requires the additional cost for the computation of SSIM, which is a little bit computationally demanding with respect to MSE. On the contrary, with respect to SSIM-NLM, ASSIM-NLM is faster since NLM (and in particular the search of similarities) runs just once while it in principle must run twice in SSIM-NLM.

Table 1 also contains the denoising results of I-ASSIM-NLM and I-MSE-NLM. A biorthogonal wavelet with odd vanishing moments is used for processing both the residual

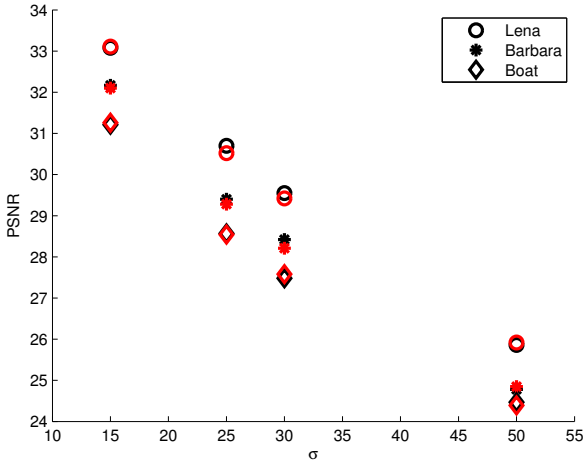

Fig. 3. PSNR results of the proposed ASSIM-NLM (dark markers) and the two step method SSIM-NLM (light markers) for three test images and different noise levels.

R and the denoised image I_d in I-ASSIM-NLM. Four scale levels of an undecimated wavelet decomposition have been fixed while in the estimation of Wiener filter coefficients, the variance of the noise is scaled according to the scale level of the transform. I-ASSIM-NLM allows us to increase the denoising result of NLM-SSIM up to $1.3db$ in terms of PSNR and up to 0.03 in terms of SSIM. In addition, the proposed method provides results that are close to those provided by BM3D for different test images. A better estimation of the corrective terms and a different weighting function would allow the proposed denoiser to be really competitive with BM3D.

4. CONCLUSIONS

In this paper a SSIM based NLM denoising method has been proposed. The method uses a corrected version of SSIM, which takes into account its sensitiveness to noisy data. This kind of correction allows us to avoid a pre-denoising step of the image to be used in the evaluation of the metric as well as better denoising results with respect to the classical NLM in terms of PSNR, SSIM and subjective visual quality. A further refinement of the denoising results can be performed on the denoised image by simply Wiener filtering both the denoised image and its residual. This kind of refinement is not costly and allows us to achieve denoising results that are close and sometimes comparable to BM3D, that actually is the most performing two-step denosing method and exploits image inner similarities for denoising. The proposed method also seems somewhat robust to some NLM parameters. Future research will be devoted to improve the correction of SSIM with a more precise estimation of the error, trying also

to embed the refinement step directly in the NLM-SSIM denoiser. In addition, the ASSIM-NLM could be used in the first step of the BM3D algorithm.

A. APPENDIX

For the estimation of the relative error, we can use the following relations from the floating point arithmetic [21]:

$$a)\ \varepsilon_{x\pm y} \approx \frac{x}{x\pm y}\varepsilon_x \pm \frac{y}{x\pm y}\varepsilon_y;$$
$$b)\ \varepsilon_{xy} \approx \varepsilon_x + \varepsilon_y; \quad c)\ \varepsilon_{\frac{x}{y}} \approx \varepsilon_x - \varepsilon_y \tag{7}$$

where x and y are two generic variables. Since $1 - S_2 = \frac{\|B_x - B_y - (\mu_x - \mu_y)\|^2}{\|B_x-\mu_x\|^2 + \|B_y-\mu_y\|^2 + C_2}$, using $c)$ and then $a)$, we have

$$\begin{aligned}\varepsilon_{1-S_2} \approx\ & \varepsilon_{\|B_x - B_y - (\mu_x-\mu_y)\|^2} + \\ -\frac{\|B_x-\mu_x\|^2}{\|B_x-\mu_x\|^2 + \|B_y-\mu_y\|^2 + C_2}&\varepsilon_{\|B_x-\mu_x\|^2} + \\ -\frac{\|B_y-\mu_y\|^2}{\|B_x-\mu_x\|^2 + \|B_y-\mu_y\|^2 + C_2}&\varepsilon_{\|B_y-\mu_y\|^2}.\end{aligned} \tag{8}$$

where $\varepsilon_{\|B_x - B_y - (\mu_x-\mu_y)\|^2} \approx \frac{2\sigma^2}{\|B_x - B_y - (\mu_x-\mu_y)\|^2}$, $\varepsilon_{\|B_x-\mu_x\|^2} \approx \frac{\sigma^2}{\|B_x-\mu_x\|^2}$ and $\varepsilon_{\|B_y-\mu_y\|^2} \approx \frac{\sigma^2}{\|B_y-\mu_y\|^2}$ in their simplest form.

REFERENCES

[1] A. Buades, B. Coll, and J. Morel, A review of image denoising algorithms, with a new one, Multiscale Mod. and Simul., vol. 4, no. 2, pp. 490-530, 2005.

[2] J. Darbon, A. Cunha, T. Chan, S. Osher, and G. Jensen, Fast nonlocal filtering applied to electron cryomicroscopy, IEEE Int. Symp. on Biomed. Imag.: From Nano to Macro, 2008, pp. 1331-1334.

[3] R. Lai and Y. Yang, Accelerating non-local means algorithm with random projection, Electronics Letters, vol. 47, no. 3, pp. 182-183, 3 2011.

[4] K. Chaudhury, Acceleration of the shiftable o(1) algorithm for bilateral filtering and non-local means, IEEE Trans. on Image Proc., 2012.

[5] R. Vignesh, B. T. Oh, and C.C. Kuo, Fast non-local means (nlm) computation with probabilistic early termination, IEEE Signal Proc. Letters, vol. 17, no. 3, pp. 277-280, mar. 2010.

[6] D. Van De Ville and M. Kocher, Sure-based non-local means, IEEE Signal Proc. Letters, vol. 16, no. 11, pp. 973-976, nov. 2009.

[7] J. Salmon, On two parameters for denoising with non-local means, IEEE Signal Proc. Letters, vol. 17, no. 3, pp. 269-272, 2010.

[8] W. Zeng and X. Lu, Region-based non-local means algorithm for noise removal, Electronics Letters, vol. 47, no. 20, pp. 1125-1127, 29 2011.

[9] P. Coupe, J. Manjon, M. Robles, and D. Collins, Adaptive multiresolution non-local means filter for three-dimensional magnetic resonance image denoising, IET Image Processing, vol. 6, no. 5, 2012.

[10] N. Thacker, J. Manjon, and P. Bromiley, Statistical interpretation of non-local means, IET Computer Vision, vol. 4, no. 3, pp. 162-172, 2010.

[11] C. Deledalle, V. Duval, and J. Salmon, Non-local methods with shape-adaptive patches (nlm-sap), Journal of Mathematical Imaging and Vision, vol. 43, no. 2, pp. 103-120, 2012.

[12] K. N. Chaudhury and A. Singer, Non-local euclidean medians, IEEE Signal Proc. Letters, vol. 19, no. 11, pp. 745-748, nov. 2012.

[13] K. Dabov, A. Foi, V. Katkovnik, and K. Egiazarian, Image denoising by sparse 3D transform-domain collaborative filtering, IEEE Trans. Image Process., vol. 16, no. 8, pp. 2080-2095, August 2007.

[14] A. Rehman and Z. Wang, SSIM-Based Non-Local Means Image Denoising, IEEE Proc. of ICIP '11, Belgium, 2011.

[15] Z. Wang and A.C. Bovik, Mean squared error: love it or leave it? - a new look at signal fidelity measures, IEEE Signal Proc. Magazine, vol. 26, pp. 98-117, Jan. 2009.

[16] Z. Wang, A. Bovik, H. Sheikh, and E.P. Simoncelli, Image quality assessment: From error visibility to structural similarity, IEEE Trans. on Image Processing, vol. 13, pp. 600-612, Apr. 2004.

[17] Y. Wu, B. Tracey, P. Natarajan and J. P. Noonan, Probabilistic Non-Local Means, IEEE Signal Proc. Letters, Vol. 20, no. 8, pp. 763-766, 2013.

[18] R. Xi, Z. Wang, X. Zhao, M. Xie, X. Wang, A non-local means based vectorial total variational model for multichannel SAR image denoising, Proc. of CISP '13, Vol. 01, pp. 234-239, 2013.

[19] B.A. Abrahim, Z.A. Mustafa, Y.M. Kadah, Modified non-local means filter for effective speckle reduction in ultrasound images, 28th National Radio Science Conference (NRSC), pp. 1-8, 2011.

[20] D. Brunet, E.R. Vrscay, Z. Wang, On the Mathematical Properties of the Structural Similarity Index, IEEE Trans. on Image Proc., vol. 21, no. 4, 2012.

[21] K.E. Atkinson, An Introduction to Numerical Analysis, J. Wiley & Sons Inc., 1988.

[22] D. Brunet, E.R. Vrscay, Z. Wang, The use of residuals in image denoising, Proc. of ICIAR 09, 2009.